Article | Received 7 May 2026; Revised 14 August 2026; Accepted 19 August 2026; Published 31 August 2026
https://doi.org/10.55092/sc20260016

Development of high-performance alkali-stabilized earthen composites reinforced with natural fibers: coupled thermal and mechanical behavior

Mohamed Char*, Youssef Khrissi and Amine Tilioua*

Department of Engineering Sciences, Faculty of Sciences and Techniques Errachidia, Moulay Ismaïl University of Meknès, Errachidia, Morocco

* Correspondence authors; E-mails: m.char.@edu.umi.ac.ma (M.C.); a.tilioua@umi.ac.ma (A.T.).

Highlights:

- Development of an innovative composite combining alkaline stabilization and reinforcement with natural fibers (fig tree, petiole, and alfa) for sustainable construction.
- Significant reduction in thermal conductivity (down to 0.32 W m^{-1} K^{-1}) as the fiber content increases, thereby improving the energy efficiency of buildings.
- Identification of an optimal fiber incorporation threshold between 2% and 3%, improving ductility and limiting the propagation of microcracks.
- Use of abundant raw materials and lignocellulosic waste, offering an eco-friendly alternative to conventional building materials.

Abstract: This study explores the development of sustainable, earth-based building materials that have been optimized using a dual approach involving alkaline stabilization and reinforcement with locally sourced natural fibers, resulting in composite materials with enhanced thermomechanical properties. The aim is to enhance the mechanical and thermophysical performance of compressed earth bricks while minimizing the environmental impact of the construction industry. Soil from south-eastern Morocco was chemically stabilized and mixed with varying percentages (0%–8%) of lignocellulosic fibers (petiole, fig tree, and alfa). Experimental results showed a reduction in bulk density of up to 30%, leading to significant improvements in thermal insulation, with minimum thermal conductivities of 0.32 W m^{-1} K^{-1} for fig tree and 0.50 W m^{-1} K^{-1} for alfa. In terms of mechanics, crack bridging was observed to have a reinforcing effect, with optimal compressive strength (6.4 MPa) and tensile strength (1.8 MPa) achieved at fiber contents between 2% and 3%. This synergy between stabilization and bio-reinforcement provides an eco-efficient, high-performance, and economically viable construction solution that is particularly well-suited to the climatic conditions of arid and semi ardi regions.

Keywords: earth bricks; natural fibers; alkaline stabilization; thermal conductivity; compressive strength; tensile strength; building materials

1. Introduction

The construction sector is currently facing significant environmental and energy challenges, driven by the urgent need to reduce greenhouse gas emissions, minimize resource consumption, and promote sustainable development. In this context, the transition to a resource-efficient built environment has become a global priority, driving the development of eco-friendly building materials with low environmental impact and improved energy performance [1]. Among these alternatives, earth-based materials are attracting renewed interest due to their availability, recyclability, and low embodied energy compared to conventional materials such as cement and fired bricks. Compressed earth blocks (CEBs) represent a promising solution for sustainable construction, particularly in arid and semi-arid regions. However, despite their environmental benefits, traditional earthen materials often suffer from limitations such as low mechanical strength, high sensitivity to moisture, and variable durability [2]. To overcome these drawbacks, several stabilization techniques have been proposed, including the use of cement, lime, or alkaline activators, as well as reinforcement strategies based on natural fibers. Recent studies have demonstrated that incorporating natural fibers into clay matrices significantly enhances their mechanical behavior by improving tensile strength, ductility, and crack resistance [3–5]. These fibers act as micro-reinforcements, filling cracks and limiting shrinkage during the drying process. Furthermore, the use of lignocellulosic fibers such as sisal, doum palm, or other agricultural residues helps to utilize local biomass resources while reducing environmental impacts [6,7]. In addition to mechanical improvements, natural fibers also influence the physical and thermal properties of earthen materials. From a thermal perspective, earthen building materials are known for their high thermal inertia, which contributes to indoor thermal comfort and energy efficiency. However, their relatively high thermal conductivity can limit their insulating performance. It has been demonstrated that the introduction of natural fibers reduces density and increases porosity, thereby improving thermal insulation properties [8,9]. This effect is mainly attributed to the low thermal conductivity of the fibers and the formation of air voids within the composite structure. Such improvements are essential for enhancing the energy performance of building, particularly in hot climates. Furthermore, life-cycle assessment studies confirm that earth-based materials reinforced with natural additives have a significantly lower environmental impact than conventional building materials, making them particularly well-suited to sustainable construction practices [10]. The incorporation of industrial byproducts or natural reinforcements further strengthens this approach by combining environmental benefits with improved mechanical performance [11]. Despite the growing body of research on fiber-reinforced earth materials, there remains a need to fully understand the combined effects of natural fiber reinforcement and stabilization techniques on thermal and mechanical properties. In particular, the synergy between locally available fibers and alternative binders, such as alkaline activators, has not yet been sufficiently explored. Consequently, this study aims to investigate the development of natural-fiber-reinforced stabilized earth bricks, with a focus on their thermomechanical properties. Particular attention is given to the influence of fiber type and content on thermal conductivity, density, and mechanical strength. This work contributes to the advancement of sustainable building materials by promoting the use of local resources and optimizing their performance for energy-efficient construction.

2. Materials and methods

2.1. Raw materials

2.1.1. Soil

The material used in this study was collected in the province of Errachidia, specifically in the Tmassint area (southeastern Morocco). The collection site is located approximately 4 km from the Oued Ziz Valley, an area characterized by specific sedimentary deposits (Figure 1). From a particle size perspective, this material is characterized by a very fine texture, which explains its widespread use in local construction due to its remarkable structural performance. The clay extracted from this region is particularly renowned for its high-water absorption capacity, which gives it excellent thermal inertia. This performance is essential in the region’s climate, where it enables structures to withstand significant daily and seasonal temperature fluctuations, thereby improving indoor temperature regulation [12].

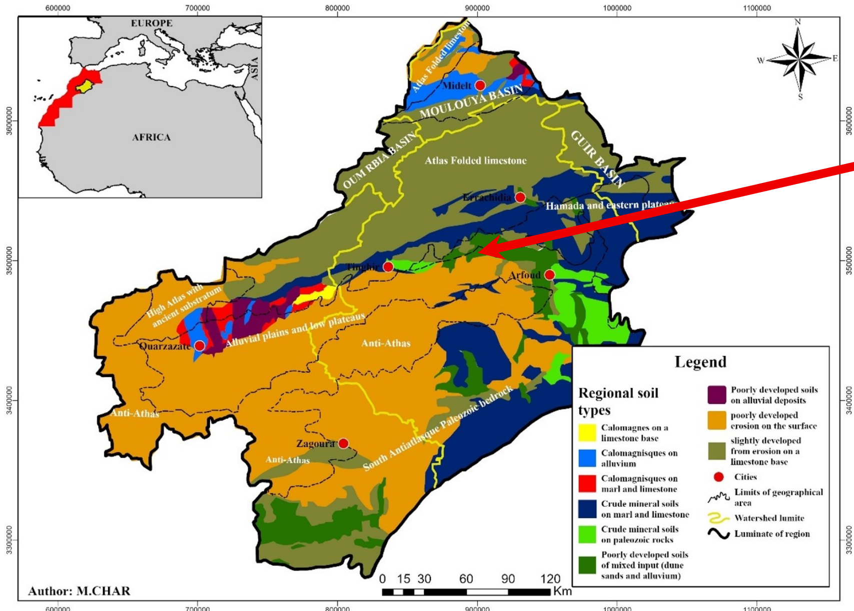

Name of soil sampling area	Location
Tmassint (Errachidia)	4 km from the Oued Ziz Valley

Figure 1. Location of soil studied.

2.1.2. Alkaline solution and natural fibers

The geopolymer synthesis, which took place between the soil matrix and the liquid phase, was carried out using commercial sodium aluminosilicate ($AlNa_{12}SiO_5$) and sodium hydroxide (NaOH). These agents, known as activating solutions, induce the formation of inorganic polymers through chemical reaction with the soil’s siliceous precursors. The resulting geopolymers are characterized by a dense crystalline structure, which gives them excellent stability against mechanical stresses and degrading agents, making them particularly durable construction materials. In this study, we used renewable natural fibers, including petiole, fig tree, and alfa fibers. The petioles were harvested in the oases of Errachidia, near the river. Fig tree and alfa fibers were obtained from fig tree and alfa waste, which was collected and cleaned before being dried for use (Figure 2a–c).

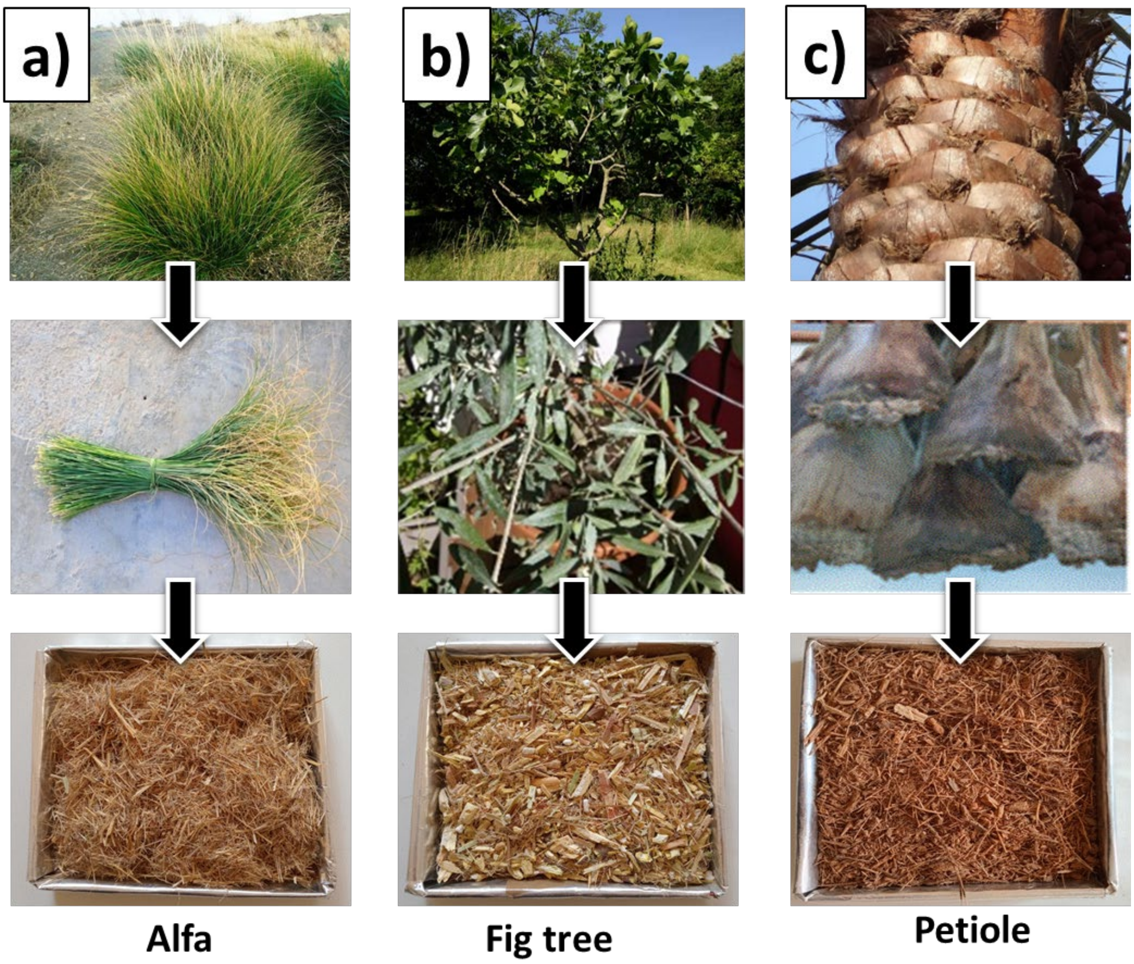

Figure 2. Process for producing plant fibers from renewable resources in the region.

The incorporation of these plant fibers (Alfa, fig tree, and petiole) into the clay matrix from the Errachidia region aims to develop eco-materials with optimized performance. This combination helps overcome the inherent fragility of raw clay by limiting cracking during drying shrinkage. By acting as a structural skeleton, the fibrous reinforcements not only improve the ductility of the final material but also enhance its thermal insulation properties thanks to the natural porosity of the cellulosic fibers. This approach is part of a sustainable construction strategy that leverages synergies between mineral resources and local biomass to address the climate challenges of the pre-Saharan region.

2.2. Experimental procedure

The sample preparation protocol involved incorporating fibers into the soil matrix at mass fractions ranging from 0% to 8%, in accordance with the proportions detailed in (Table 1). Subsequently, the liquid phase, composed of water and an activator solution, was introduced while maintaining an optimal concentration of 1.5% alkali agent by weight of water. After thorough manual mixing, the bricks were formed by compacting the mixture in molds of specific dimensions (Figure 3).

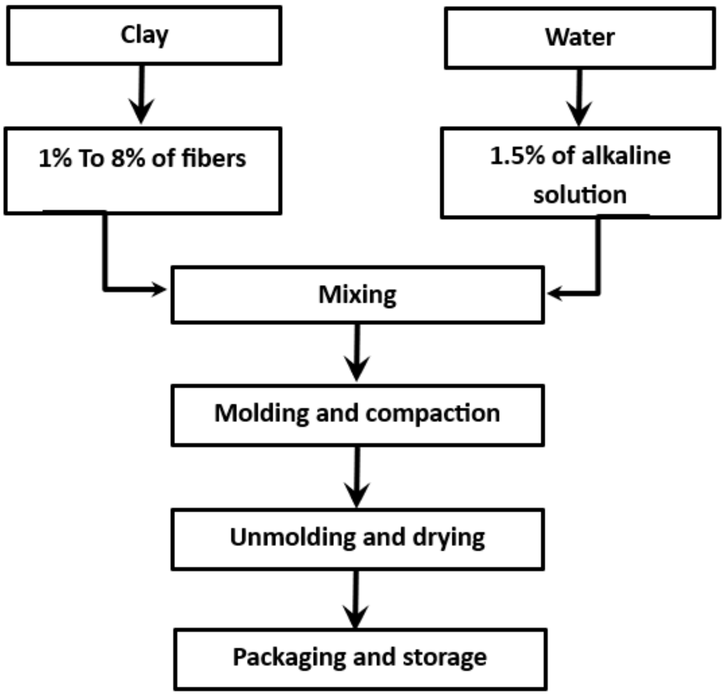

Figure 3. Composite materials manufacturing process.

The test specimens were formed using two types of molds, selected to suit the subsequent characterization protocols: prismatic molds measuring 24 × 24 × 4 cm³ for thermal testing, and cylindrical molds (D = 10 cm, H = 20 cm) for mechanical testing. The preparation of the mixtures involved incorporating fiber mass fractions ranging from 0% to 8% into the earthen matrix. The liquid phase, including mixing water and the activator solution, was then introduced while maintaining a constant optimal alkaline concentration of 1.5% relative to the water mass.

Table 1. Preparation of composite samples of clay and natural fibers.

Sample code	Percentage of clay %	Percentage of fibers %
S_0	100%	0% of (Petiole, Alfa, and Fig tree)
$S_{C.1}$, $S_{R.1}$, $S_{O.1}$	99%	1% of (Petiole, Alfa, and Fig tree)
$S_{C.2}$, $S_{R.2}$, $S_{O.2}$	98%	2% of (Petiole, Alfa, and Fig tree)
$S_{C.3}$, $S_{R.3}$, $S_{O.3}$	97%	3% of (Petiole, Alfa, and Fig tree)
$S_{C.4}$, $S_{R.4}$, $S_{O.4}$	96%	4% of (Petiole, Alfa, and Fig tree)
$S_{C.5}$, $S_{R.5}$, $S_{O.5}$	95%	5% of (Petiole, Alfa, and Fig tree)
$S_{C.6}$, $S_{R.6}$, $S_{O.6}$	94%	6% of (Petiole, Alfa, and Fig tree)
$S_{C.7}$, $S_{R.7}$, $S_{O.7}$	93%	7% of (Petiole, Alfa, and Fig tree)
$S_{C.8}$, $S_{R.8}$, $S_{O.8}$	92%	8% of (Petiole, Alfa, and Fig tree)

It should be noted that specimen dimensions (24 × 24 × 4 cm³ for thermal testing; D = 10 cm, H = 20 cm for mechanical testing) were dictated by the geometry of the specific laboratory apparatus used (PHYWE thermal box and FORM TEST SEIDNER hydraulic press, respectively) (Figure 4), rather than by a formal ASTM/ISO standard. This equipment and its associated steady-state measurement protocol have been previously validated in several peer-reviewed studies [13–15], with a reported thermal conductivity uncertainty of less than 10%, ensuring reliable and reproducible results despite the non-standardized specimen geometry.

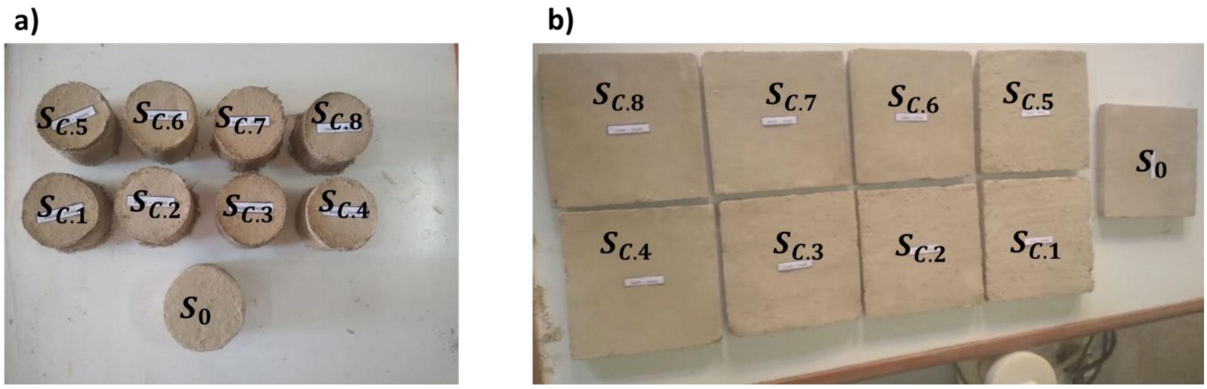

Figure 4. Set of samples studied. **(a)** To measure thermal conductivity; **(b)** To measure compressive and tensile strength.

The thermal conductivity of the samples was determined using a “thermal house” experimental setup (Figure 5). This system, consisting of a 40 × 40 × 40 cm³ cubic chamber with interchangeable walls, is well documented for the thermal evaluation of building materials, with a measurement uncertainty of less than 10% [13,14]. The chamber includes four 21 × 21 cm² side openings, sealed with 5 cm-thick expanded polystyrene panels to ensure optimal insulation. The heat flux is generated by a 100 W incandescent lamp, housed in a black box to minimize radiation losses. A thermal controller maintains a constant internal temperature of 50 °C, while the laboratory environment is stabilized at 20 °C by an air conditioning system. For each test, the 24 × 24 × 4 cm³ test specimen is mounted on one of the four lateral openings, replacing the corresponding polystyrene panel, so that one face of the specimen is exposed to the internally heated air. In contrast, the opposite face is exposed to the external ambient air. The three remaining openings are kept sealed with polystyrene panels to prevent parasitic heat loss and force heat flow through the sample. Thermocouples monitor internal and external temperature gradients. (accuracy of ± 0.7 °C) connected to a data acquisition system. Thermal conductivity is estimated once steady-state conditions are reached, generally after 6 hours of heating. The calculation is based on the principle of conservation of heat flux, considering heat transfer by convection (air-wall) and by conduction through the material, according to Equation (1):

$$\varphi = h_{\text{int}}\left(T_{loc} - T_{int}\right) \times S = S \times \lambda \times \frac{T_{int} - T_{ext}}{e} = h_{ext} \times \left(T_{ext} - T_{amb}\right) \times S \quad (1)$$

Thermal conductivity (λ) was calculated using Equations (2) and (3) with a heat transfer coefficient of 8.1 W·m⁻²·K⁻¹ [14,15]. The thermal conductivity of the samples studied was evaluated using the manufacturer’s prescribed methodology (PHYWE). This procedure involves using a PHYWE thermal control stand and a set of thermocouples to monitor temperature fluctuations inside and outside the thermal chamber [16]. Temperatures were recorded once the thermocouples had stabilized, ensuring that the system was close to equilibrium (approximately 8 hours after the start of the measurement).

$$h_{int} \times \left(T_{loc} - T_{int}\right) = \frac{\lambda}{e} \times \left(T_{int} - T_{ext}\right) \quad (2)$$

$$\lambda = e \times h_{int} \times \frac{\left(T_{loc} - T_{int}\right)}{\left(T_{int} - T_{ext}\right)} \quad (3)$$

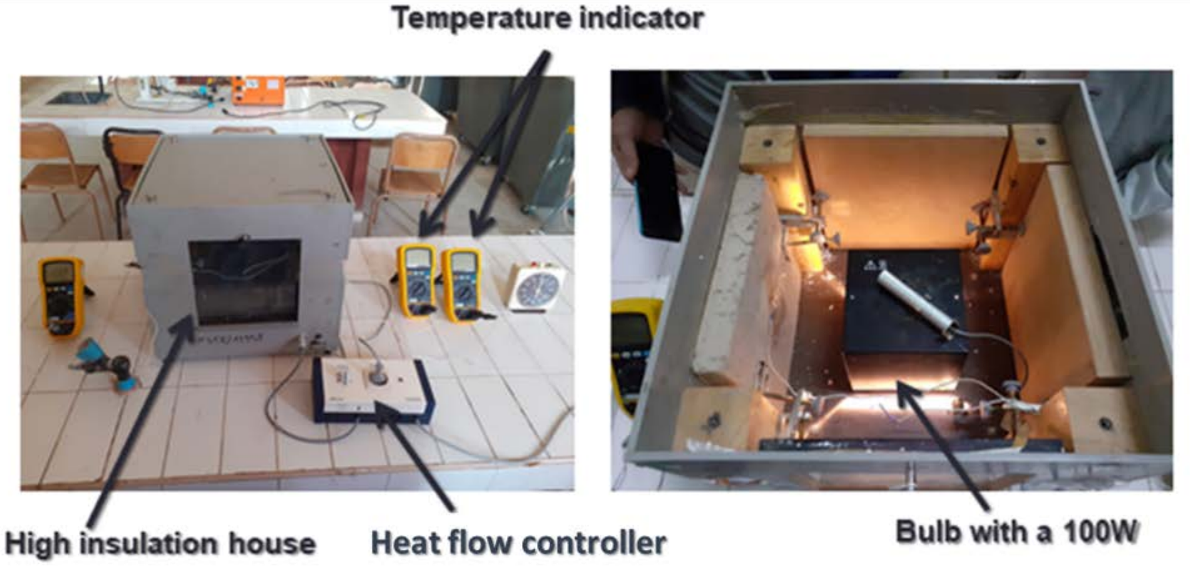

Figure 5. Thermal house.

The compressive and tensile strengths of the test specimens were evaluated using a FORM TEST SEIDNER hydraulic press (Figure 6). The device allows for the application of a controlled mechanical load, measured by a built-in high-precision force sensor. As part of this study, which focused on alkaline-stabilized earthen bricks reinforced with fig tree, alfa, and petiole fibers, stress data were digitally recorded in real time. These breaking load measurements were then used as the basis for calculating the mechanical stress, defined according to Equation (4):

$$\text{Mechanical strength} = \frac{\text{Applied force}}{\text{Sample surface}} = \frac{F}{r^2 \times \pi} \tag{4}$$

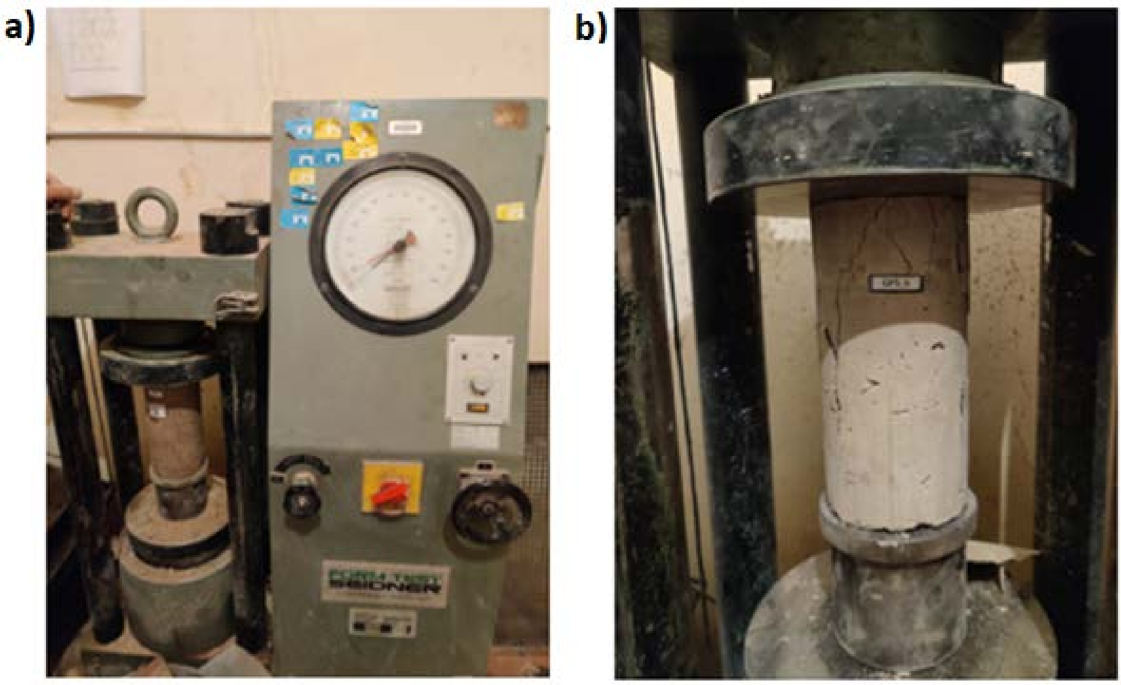

Figure 6. (a) SEIDNER FORM TEST 500KN hydraulic press; **(b)** Sample studied.

3. Results and discussion

3.1. Physicochemical, mineralogical, and morphological characterization of raw materials

3.1.1. Particle size characterization and plasticity properties of the soil

The soil's particle size distribution, as shown in (Figure 7), enables the characterization of its textural composition. The experimental data reveal a predominance of fine particles, ranging from 0.002 mm to 0.65 mm, thus confirming a low proportion of coarse particles. This fine-grain size distribution plays a decisive role in the material's mechanical properties, its reactivity to binders, and its shrinkage kinetics during drying. Consequently, this analysis is an essential prerequisite for evaluating the soil's suitability for stabilization and predicting its structural performance. The study of the soil's clay fraction made it possible to define its consistency states by determining the Atterberg limits.

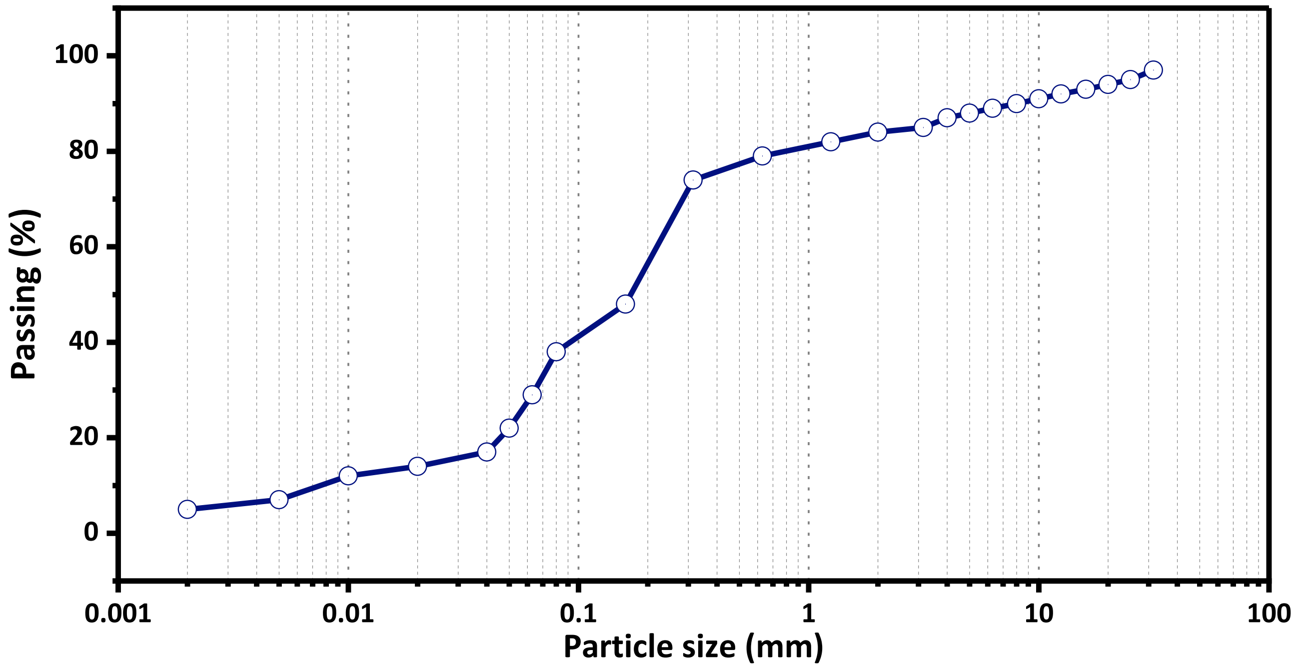

Figure 7. Particle size analysis of the studied soil.

The identified parameters, namely the liquid limit (WL), the plastic limit (WP), and the plasticity index (IP = WL − WP), are listed in Table 2. A detailed characterization of these hydraulic properties is essential, as it allows for the prediction of the material's mechanical response based on its water content, which determines its overall technical behavior and workability.

Table 2. Classification of the studied soil with respect to plasticity using the Atterberg limits [17].

W_L (%)	W_P (%)	I_P (%)	Soil Plasticity	Swelling potential	Recommended Technique
39	23	16	Medium	Medium	CEB/A

3.1.2. Mineralogical analysis of raw materials by X-ray diffraction

XRD analysis makes it possible to distinguish crystalline phases (cellulose) from amorphous phases (lignin and hemicelluloses) within lignocellulosic fibers, whose typical composition ranges from 40 % to 60 % cellulose [18]. The X-ray diffraction patterns recorded for alfa, petiole, and fig tree fibers (Figure 8) exhibit structural profiles characteristic of native cellulose (cellulose I). Two distinct features define these diffraction patterns: a primary crystalline peak appearing between 2θ = 21° and 23°, and a diffuse amorphous halo centered around 2θ = 15°, which reflects the presence of non-crystalline components, such as lignin and hemicelluloses, consistent with previous studies [19–21].

A comparative analysis of the spectra reveals a clear hierarchy in the relative crystallinity of the samples. Alfa fiber exhibits the most defined and narrowest reflection at 22°, suggesting a highly organized molecular arrangement. In contrast, petiole fiber exhibits a broader profile, indicating a more dominant amorphous phase, while fig fiber exhibits an intermediate structural state. These morphological variations, which are intrinsically linked to specific cellulose-to-lignin ratios, directly determine the physical behavior of the fibers. A high degree of crystallinity, as observed in the alpha fiber, improves mechanical stiffness, while the increased amorphous phase content in the petiole fiber promotes greater ductility and flexibility.

X-ray diffraction (XRD) analysis of the soil sample (Figure 9) reveals a mineralogical composition dominated by well-defined crystalline phases, characterized by intense, narrow peaks, indicating good overall crystallinity and a low proportion of amorphous material. Quantitative interpretation Table 3 reveals that this soil is composed primarily of calcite (43.33%), quartz (36.51%), dolomite (16.18%), and muscovite (3.98%). The characteristic peaks observed at 29.4° and 26.6° comfirm the dominant presence of calcite and quartz, respectively, indicating a carbonate-based soil with a significant siliceous fraction. The presence of dolomite suggests formation conditions rich in magnesium, while muscovite, although present in small quantities, reveals a low contribution of phyllosilicates, indicating that the material has a low clay content. This mineralogical composition confers the soil specific physicochemical properties: good mechanical and chemical stability due to the presence of quartz, as well as a relatively high volumetric heat capacity attributed to the carbonates. The low clay content, however, limits hygroscopicity. This soil therefore exhibits intermediate thermal behavior: the carbonate fraction promotes thermal storage, while the siliceous phase tends to increase thermal conductivity, which is a key parameter for its potential use in composite materials intended for insulation.

Table 3. Results of the X-ray diffraction analysis of the soil under study.

Compound Name	Chemical Formula	Sample and Mineral percentages (%)
Calcite	$Ca\,(CO_3)$	43.33
Quartz	SiO_2	36.51
Dolomite	$CaMg\,(CO_3)_2$	16.18
Muscovite	$H_2KAl_3Si_3O_{12}$	3.98

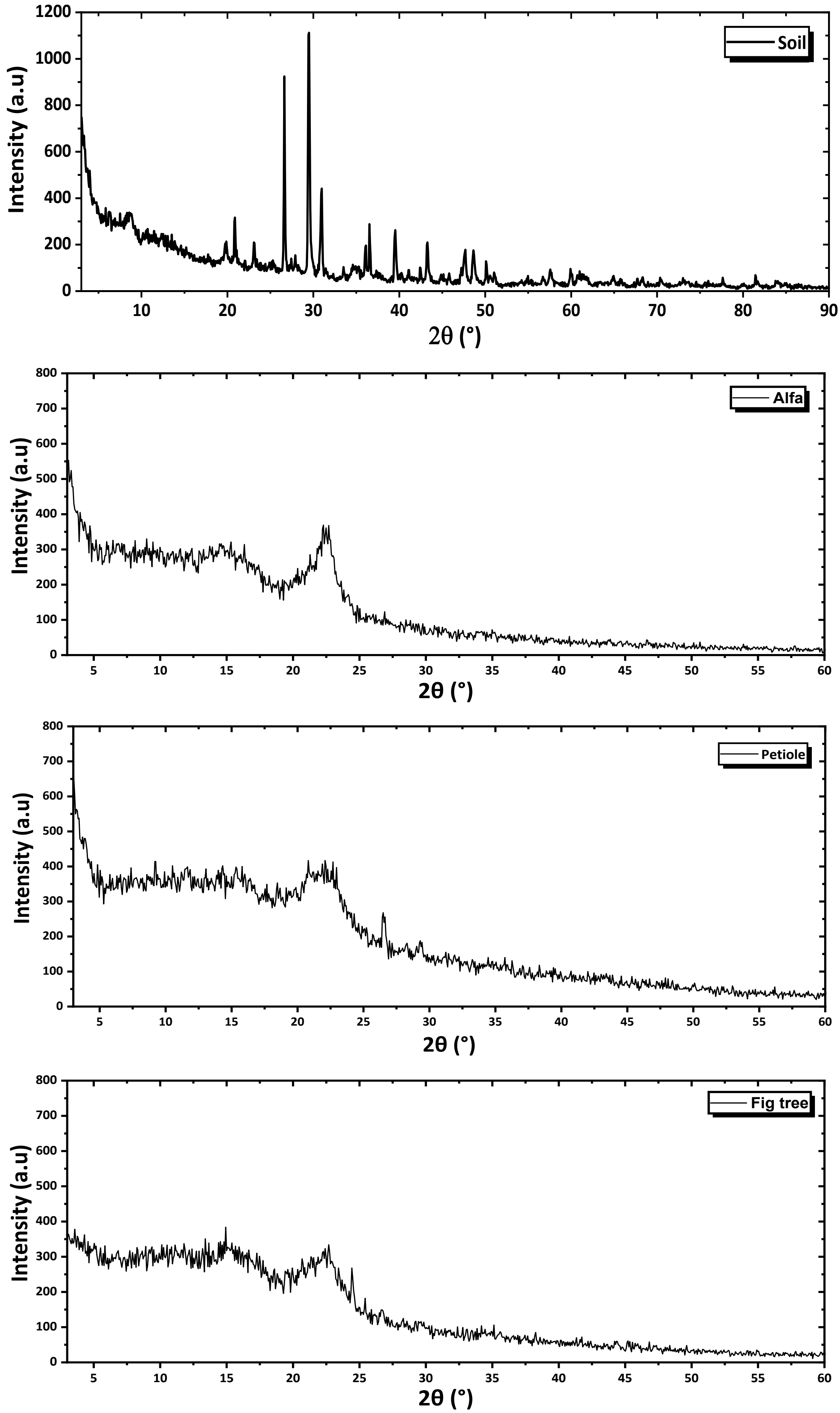

Figure 8. XRD analysis results for the raw materials used.

In conclusion, this X-ray diffraction study confirms the semi-crystalline nature of the fibers studied and highlights the decisive influence of their internal organization on their final properties, which is consistent with previous studies [22,23].

3.1.3. Structural analysis of raw materials by Fourier-transform infrared spectroscopy

Fourier-transform infrared spectroscopy (TIR)analysis identified the main functional groups present in the soil and plant fibers studied. For the soil (Figure 9), the spectrum reveals a predominantly mineral composition.

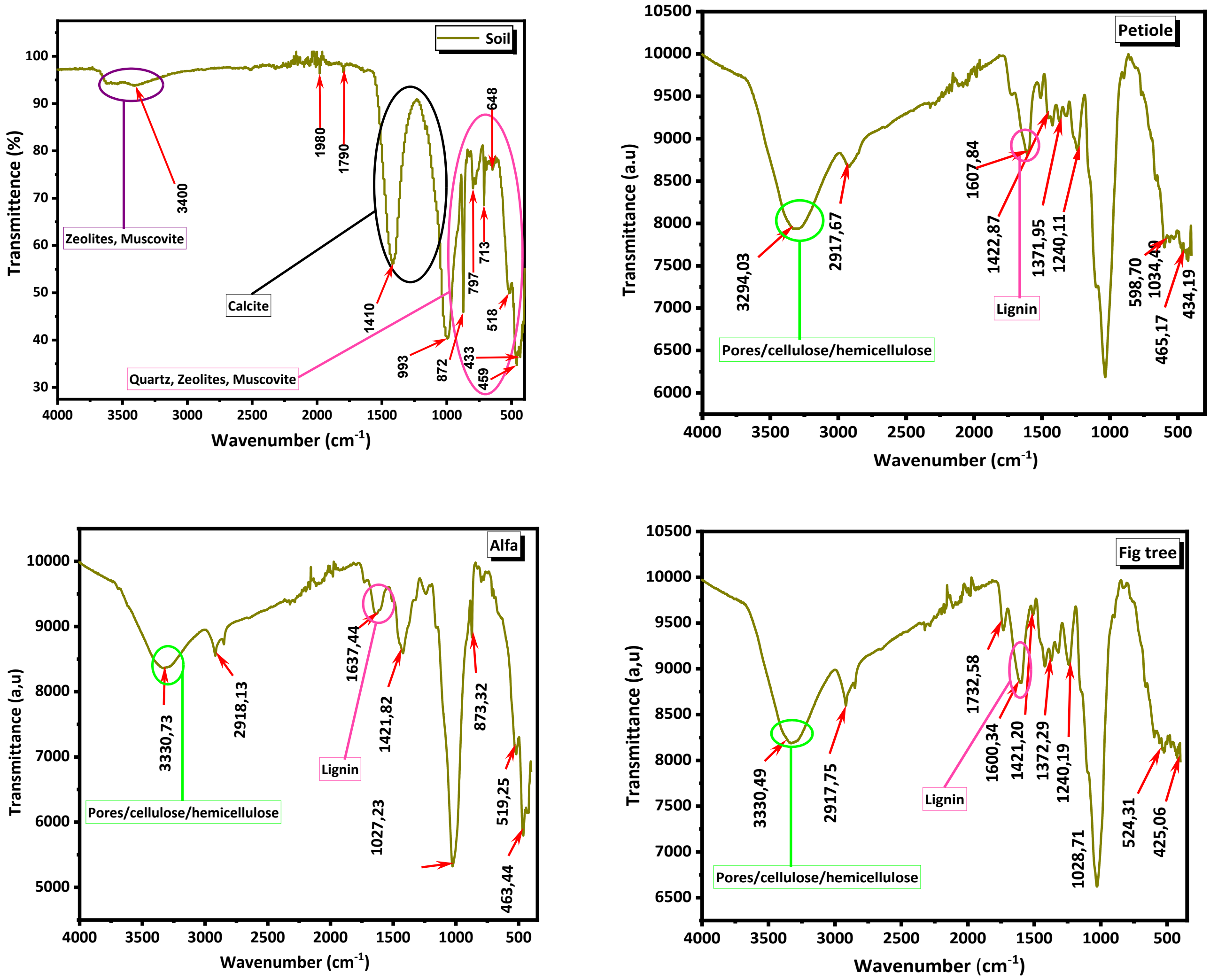

Figure 9. FTIR analysis results for the raw materials used.

Distinct bands at 1410 cm^{-1} and 872 cm^{-1} indicate the presence of calcite ($CaCO_3$). Other peaks, observed around 993 cm^{-1}, 797 cm^{-1}, and between 433 and 518 cm^{-1}, confirm the presence of quartz and various silicates, such as zeolites and muscovite [24]. As for the plant fibers (fig tree, esparto grass, and petiole), the spectra exhibit characteristics typical of lignocellulosic materials [25–29]. A broad band between 3294 and 3330 cm^{-1} is associated with hydroxyl (-OH) groups, while the peaks observed around 2917 and 2918 cm^{-1} correspond to C-H bonds. The bands observed between 1600 and 1637 cm^{-1} as well as at 1421 cm^{-1} are associated with lignin, while the peak located around 1027–1034 cm^{-1} is characteristic of cellulose. Overall, these results confirm that the soil is primarily mineral in nature, while the fibers are rich in organic compounds, particularly cellulose. This complementarity makes them suitable for joint use in the manufacture of bio-based composite materials.

3.1.4. Morphological and compositional analysis of raw materials by SEM-EDX

Microscopic examination, combined with targeted chemical analysis, allows for the precise characterization of the surface condition and composition of the components of the future composite. The micrograph of the studied soil (Figure 10a) shows a heterogeneous, aggregated structure. Particles of various geometric shapes are clearly distinguishable: rhombohedral clusters corresponding to calcite and more angular grains identified as quartz, which is in perfect agreement with the previous XRD and FTIR analyses. This mineral composition is confirmed by the overall energy-dispersive X-ray spectroscopy (EDX) analysis presented in (Table 4). The spectrum reveals a predominance of oxygen (54.47% by mass) and silicon (12.41%), the major constituent elements of the silicate fraction (quartz, clays). The high calcium content (14.00%) confirms the strongly carbonated nature of this carbonated soil from Errachidia, while the presence of aluminum (5.79%), iron (3.66%), and potassium (1.78%) indicates the presence of clay phases (illite, *etc.*).

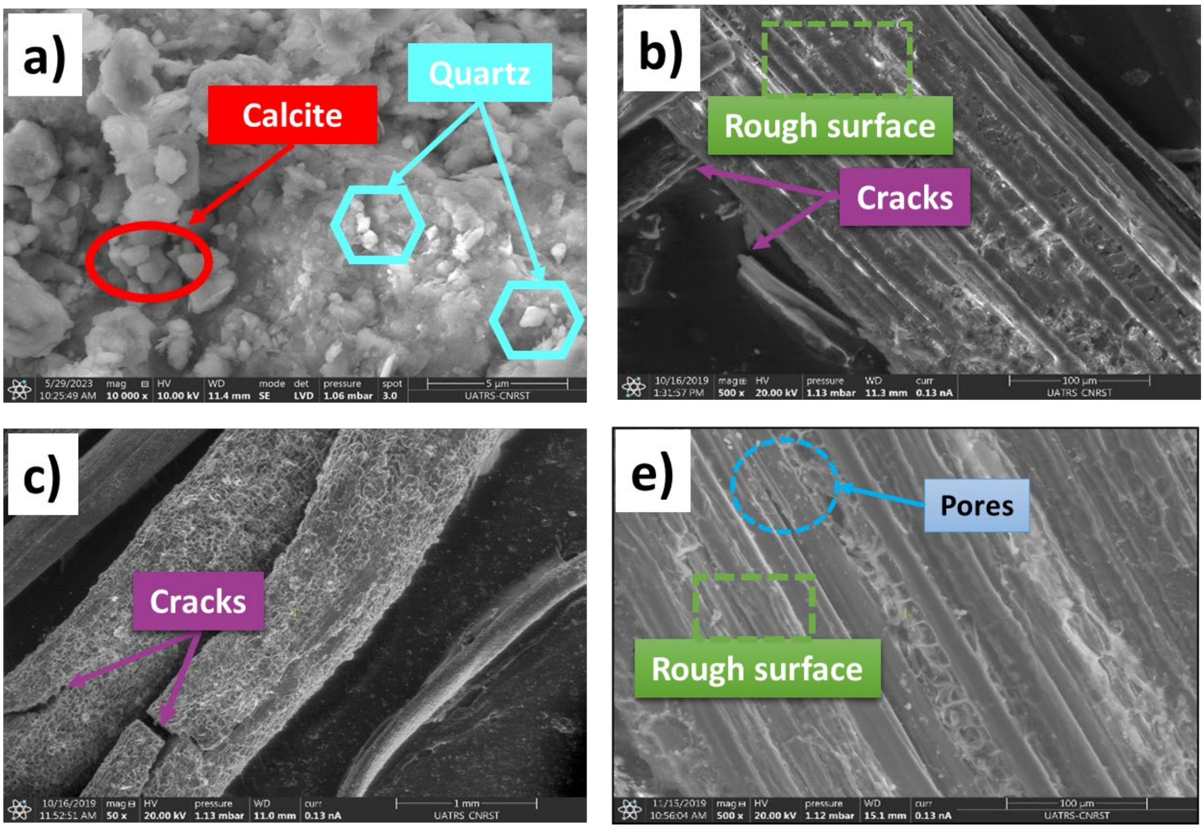

Figure 10. Scanning Electron Microscope (SEM) images of raw materials. **(a)** Soil; **(b)** Alfa; **(c)** Petiole; **(e)** Fig tree.

Observation of the plant fibers reveals distinct surface topographies that will influence adhesion to the clay matrix.

(1) The alfa fiber (Figure 10b) has a longitudinally striated surface, dotted with fissures and areas of marked roughness. This rough texture is, in principle, conducive to significant mechanical bonding.

(2) The petiole (Figure 10c) has a coarser, bundle-like structure, marked by distinct transverse fissures. Its surface appears less cohesive than that of the esparto.

(3) The fig tree (Figure 10e) has a complex morphology, with a rough surface and numerous pores or cavities. This porosity could facilitate the infiltration of the fine clay paste during mixing, thereby creating microscopic anchors.

Table 5 presents the O/C element ratios determined by EDX on the fibers. These values, ranging from 1.53 for the petiole to 1.66 for alfa, are characteristic of lignocellulosic materials.

Table 4. EDX analysis results for the soil sample.

Element	Weight %	Atom %
C	5.01	8.26
O	54.47	67.45
Na	0.40	0.34
Mg	1.93	1.57
Al	5.79	4.25
K	1.78	0.90
Ti	0.47	0.19
Fe	3.66	1.30
Ca	14.00	6.92
Cl	0.10	0.06
Si	12.41	8.75
Total	**100.00**	**100.00**

They reflect the relative abundance of oxygen-containing compounds (cellulose, hemicelluloses) compared to lignin, which is richer in carbon. Alfa has the highest O/C ratio, which could be related to its more pronounced cellulose crystallinity observed by XRD, while the petiole, with the lowest ratio, suggests a slightly higher amorphous content. These data confirm the organic nature and reinforcing potential of these local biological resources.

Table 5. Oxygen/carbon ratios of the plant fibers studied.

Plant fibers	Carbone (C) %	Oxygen (O) %	Remaining elements %	Rapport O/C
Petiole	37.60	57.55	4.85	1.53
Alfa	35.94	59.61	4.45	1.66
Fig tree	37.15	58.48	4.37	1.57

3.2. Thermal conductivity and thermal resistance

The results of this study highlight the significant influence of incorporating fig, petiole, and alfa fibers, as well as alkaline stabilization, on the thermophysical performance of earthen bricks. For all tests, the concentration of the activating solution was kept constant at 1.5% by mass relative to the mixing water.

As shown in (Figure 11), the thermal conductivity of the stabilized bricks decreases progressively as the reinforcement content increases. For composites incorporating fig tree fibers, the thermal conductivity drops from 0.702 W m^{-1} K^{-1} (control without fibers) to 0.32 W m^{-1} K^{-1} at an 8% dosage. This decrease follows a nearly monotonic trend, with intermediate values of 0.70, 0.642, 0.60, 0.58, 0.42, 0.41, and 0.38 W m^{-1} K^{-1}, correlated with the increase in the fiber percentage. Similarly, at an 8% content, bricks reinforced with petiole and alfa fibers exhibit thermal conductivities of 0.566 W m^{-1} K^{-1} and 0.501 W m^{-1} K^{-1}, respectively. These differences confirm that the intrinsic nature of the fibers influences overall thermal performance, due to their differences in microstructure, internal porosity, and lignocellulosic composition.

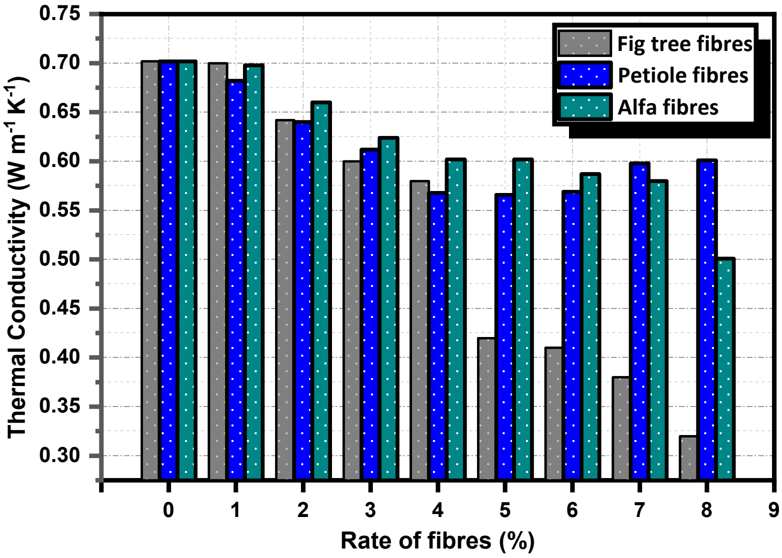

Figure 11. Variation in thermal conductivity as a function of fiber content.

Furthermore, Figure 12 shows that thermal resistance varies inversely with thermal conductivity, increasing significantly with fiber content. This structural improvement is explained by the creation of pores and air voids within the earthen matrix, induced by the insertion of fibers. These air inclusions, characterized by extremely low thermal conductivity, act as insulating barriers that limit the propagation of heat flow through the material [30–32]. These observations are consistent with the specialized literature, which highlights the beneficial effect of natural fibers on the insulating properties of building materials [33,34]. The introduction of bio-resources helps reduce bulk density while increasing porosity, two key parameters of thermal efficiency. Ultimately, the incorporation of fig, petiole, and alfa fibers into alkali-stabilized earth bricks results in a significant reduction in thermal conductivity coupled with an increase in thermal resistance. These results confirm the strong potential of these eco-composites for applications in sustainable construction, promoting the energy efficiency of buildings.

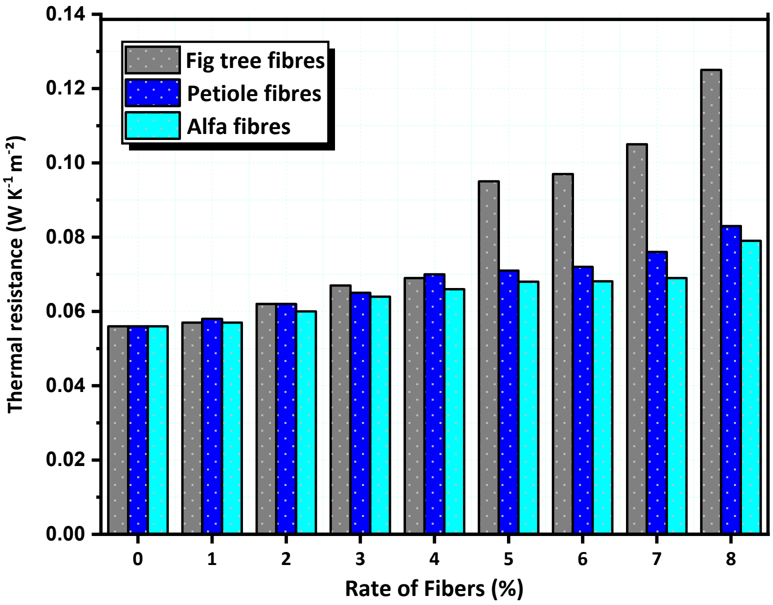

Figure 12. Variation in thermal resistance as a function of fiber content.

3.3. Mechanical compressive and tensile strength

The results of mechanical tests conducted on unstabilized and unreinforced earthen bricks show relatively low strengths, with a compressive strength of 4.2 MPa and a tensile strength of 0.82 MPa (Figures 13 and 14). These values are characteristic of raw earthen materials, whose brittleness is primarily due to their porous structure and low intergranular cohesion.

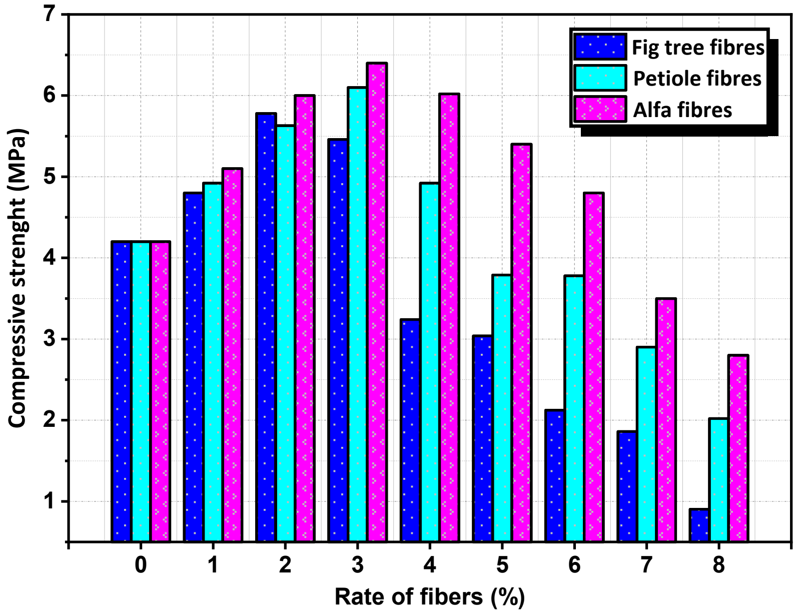

Figure 13. Variation in compressive strength as a function of fiber content.

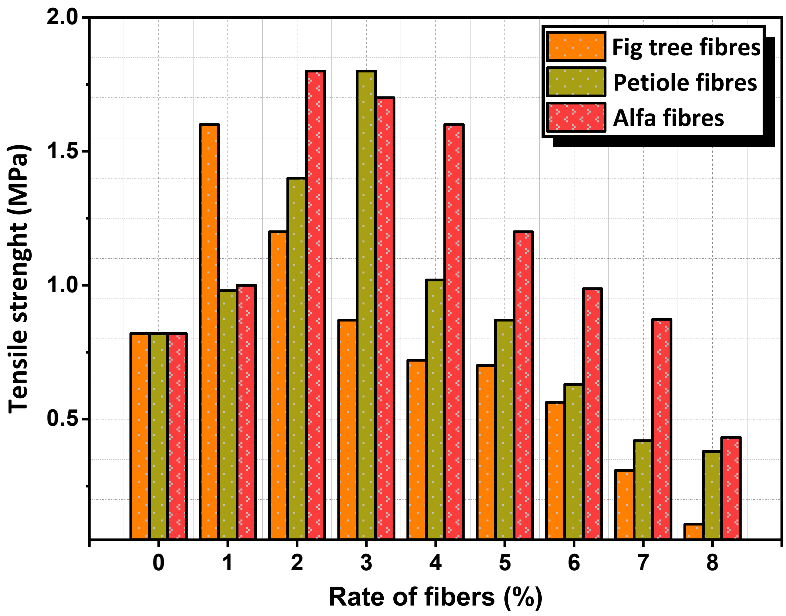

Figure 14. Variation in tensile strength as a function of fiber content.

The incorpration of natural fibers, combined with alkaline activation, leads to a significant improvement in mechanical performance. This improvement is directly linked to the role of the fibers in the matrix, particularly their ability to act as crack bridges, thereby limiting the initiation and propagation of microcracks under load. For fig tree fibers, compressive strength increases up to 5.78 MPa at an optimal fiber content of 2%, then decreases beyond that. Tensile strength reaches a maximum of 1.6 MPa at 1% fiber content. This trend reflects a good reinforcing effect at low fiber content, which is rapidly limited by matrix disorganization at higher concentrations. Petiole fibers exhibit superior performance, with a compressive strength of up to 6.1 MPa at a fiber content of 3% and a tensile strength of 1.8 MPa. This improvement suggests better fiber-matrix interaction and increased efficiency in stress transfer. Alfa fibers demonstrate the best overall performance. Compressive strength reaches 6.4 MPa at a 2% fiber content, while maximum tensile strength (1.8 MPa) is achieved at 3%. These results indicate a more effective mechanical contribution, likely due to better interfacial adhesion and favorable fiber morphology.

The improvement in mechanical properties can be explained by several mechanisms:

(1) Crack bridging: the fibers delay the initiation and propagation of cracks, thereby increasing the tensile strength and ductility of the material.
(2) Stress transfer: the fibers ensure a redistribution of stresses within the matrix, reducing local stress concentrations.
(3) Improved internal cohesion: fiber-matrix interaction helps reinforce the overall structure of the composite.

Despite these positive effects, a decrease in performance is observed beyond a certain fiber content (between 2% and 3%, depending on the type). This decline can be explained by:

(1) Increased porosity due to an excess of fibers.
(2) Poor dispersion leading to heterogeneous zones.
(3) Reduced matrix cohesion, as the fibers disrupt contact between the clay particles.

These results highlight the existence of an optimal incorporation rate, beyond which the reinforcing effect becomes counterproductive. Overall, the addition of natural fibers significantly improves the mechanical performance of clay bricks, particularly their tensile strength, which is generally low in unreinforced materials. Among the fibers studied, alfa fibers appear to be the most effective, followed by petiole fibers, and then fig tree fibers. These observations confirm that the choice of fiber type and content is a key parameter in the design of earth-based composite materials. They are consistent with previous work showing that plant fibers represent a promising solution for improving the durability, strength, and ductility of eco-friendly building materials [35–37].

3.4. Effect of natural fibers on the density of stabilized earth bricks

As shown in Table 6, the incorporation of natural fibers (petiole, alfa, and fig tree) leads to a gradual decrease in the bulk density of stabilized earth bricks. The density of the reference sample without fibers is 1682 kg/m^3, while adding 8% fibers reduces it to approximately 1150–1160 kg/m^3, a decrease of about 30%. This reduction is mainly attributed to the lower intrinsic density of lignocellulosic fibers compared to the mineral matrix, as well as their porous cellular structure, characterized by internal cavities (lumens) [38].

Table 6. Variation in the apparent density of earth bricks reinforced with different natural fibers and stabilized with an alkaline solution, depending on the fiber content.

Fiber Percentage	Density with Petiole fibers (kg/m³)	Density with Alfa fibers (kg/m³)	Density with Fig tree fibers (kg/m³)
0%	1682.0	1682.0	1682.0
1%	1610.5	1611.0	1608.3
2%	1579.0	1580.0	1575.0
3%	1514.5	1517.0	1511.2
4%	1471.0	1473.0	1467.0
5%	1368.5	1370.0	1362.6
6%	1315.0	1317.0	1308.0
7%	1261.5	1264.0	1254.7
8%	1156.0	1160.0	1151.0

In addition, the introduction of fibres disrupts the compactness of the clay-sand matrix and promotes the formation of interfacial voids between the fibers and the matrix, thereby increasing the composite's internal porosity and reducing bulk density [39]. As shown in Table 6, the differences observed between fiber types remain relatively small for the same incorporation rate, suggesting that the volume fraction of fibers is the dominant factor in density variation. This decrease in density is particularly interesting for the development of bio-based building materials, as it is generally associated with improved thermal insulation performance, driven by increased porosity and the presence of trapped air in the material's microstructure [40].

4. Conclusion

This study demonstrates the effectiveness of combining alkaline stabilization with natural fiber reinforcement to develop earth-based construction materials that are both durable and high-performing. The main results and implications can be summarized as follows:

(1) The incorporation of lignocellulosic fibers (petiole, fig tree, alfa) significantly reduces the bulk density of the bricks (by up to 30%) and their thermal conductivity (reaching 0.32 W m^{-1} K^{-1} for fig tree), thanks to increased porosity and the insulating properties of the fibers.

(2) The fibers act as crack bridges, improving compressive and tensile strength up to an optimal threshold of 2%–3%. Beyond this threshold, excess fibers impair matrix cohesion. Alfa fibers demonstrated the best mechanical performance (6.4 MPa in compression, 1.8 MPa in tension).

(3) Alkaline stabilization improves the cohesion and durability of the clay matrix, while the fibers provide structural reinforcement and thermal efficiency. This synergy creates a composite whose overall performance surpasses that of traditional, unstabilized earthen bricks.

(4) The stabilized and reinforced earth bricks developed in this research represent an environmentally friendly and economically viable solution, particularly suited to regions rich in local resources and arid climates.

(5) For larger-scale application, future research should focus on studying long-term durability, hygrothermal behavior, and optimizing fiber surface treatments to improve adhesion at the fiber-matrix interface and the material's longevity.

Data availability statement

No supplementary or additional data were generated in this study.

Declaration of generative AI and AI-assisted technologies

During the preparation of this manuscript, the authors used generative AI tools only to improve language and readability. Specifically, the authors used DeepL, Grammarly for translation in limited sections. The authors take full responsibility for the content of the manuscript.

Acknowledgments

We sincerely thank the CNRST (National Center for Scientific and Technical Research - Morocco) for supporting the essential analyses for this research. Our gratitude extends to Moulay Ismail University of Meknès, Morocco, for its continuous support and available facilities throughout this project.

Authors' contribution

Writing—original draft, visualization, software, resources, methodology, investigation, formal analysis, data curation, conceptualization: M.C.; writing—review and editing, methodology, investigation, formal analysis, data curation, conceptualization: Y.K.; writing—review and editing, visualization, validation, supervision, software, resources, project administration, methodology, investigation, data curation, conceptualization: A.T. All authors have read and agreed to the published version of the manuscript.

Conflicts of interest

The authors declare no conflicts of interest.

References

[1] Ness DA, Xing K. Toward a resource-efficient built environment: a literature review and conceptual model. *J. Ind. Ecol.* 2017, 21(3):572–592.
[2] Oti JE, Kinuthia JM, Bai J. Engineering properties of unfired clay masonry bricks. *Eng. Geol.* 2009, 107(3–4):130–139.
[3] Latha AT, Murugesan B, Thomas BS. Compressed earth block reinforced with sisal fiber and stabilized with cement: manual compaction procedure and influence of addition on mechanical properties. *Mater. Today Proc.* 2023.
[4] Jesudass A, Gayathri V, Geethan R, Gobirajan M, Venkatesh M. Earthen blocks with natural fibres-a review. *Mater. Today Proc.* 2021, 45:6979–6986.
[5] Bougtaib K, Jamil Y, Nasla S, Gueraoui K, Cherraj M. Compressed earth blocks reinforced with fibers (doum palm) and stabilized with lime: manual compaction procedure and influence of addition on mechanical properties and durability. *JP J. Heat Mass Transfer.* 2022, 26:157–177.
[6] Ojo EB, Bello KO, Mustapha K, Teixeira RS, Santos SF, *et al.* Effects of fibre reinforcements on properties of extruded alkali activated earthen building materials. *Constr. Build. Mater.* 2019, 227:116778.

[7] Char M, Khrissi Y, Tilioua A, Development of ecological thermal insulation materials based on renewable natural fiber waste and gum arabic: experimental study and characterization for use in semi-arid climates. *Results Eng*. 2025, 27:106510.
[8] Bouchefra I, Bichri FE, Chehouani H, Benhamou B. Mechanical and thermophysical properties of compressed earth brick reinforced by raw and treated doum fibers. *Constr. Build. Mater.* 2022, 318:126031.
[9] Saidi M, Cherif AS, Zeghmati B, Sediki E. Stabilization effects on the thermal conductivity and sorption behavior of earth bricks. *Constr. Build. Mater.* 2018, 167:566–577.
[10] Mateus R, Fernandes J, Teixeira ER. *Environmental Life Cycle Analysis of Earthen Building Materials*. Amsterdam: Elsevier, 2019.
[11] Ganesh CR, Sumalatha J, Sreekeshava KS, Sharath K. Experimental study on strength behaviour of geofibre reinforced stabilized mud blocks using industrial by-products. *Mater. Today Proc.* 2023.
[12] Annaba K, Belarouf S, Wardi FZ, Ibaaz K, Cherkaoui M, *et al*. Harnessing natural pozzolan for sustainable heating and cooling: thermal performance and building efficiency in moroccan climates. *Buildings* 2024, 14(9):2633.
[13] Silva FJG, Baptista A, Pinto G, Campilho RD, Ribeiro MCS. Characterization of hybrid pultruded structural products based on preforms. *Compos. B Eng.* 2018, 140:16–26.
[14] Navacerrada MA, Fernandez P, Díaz C, Pedrero A. Thermal and acoustic properties of aluminium foams manufactured by the infiltration process. *Appl. Acoust.* 2013, 74(4):496–501.
[15] Benallel A, Tilioua A, Mellaikhafi A, Babaoui A, Hamdi MA. Thermal characterization of insulating materials based on date palm particles and cardboard waste for use in thermal insulation building. In P*roceedings of the AMT2020: the 6th international congress on thermal sciences*, Online, April 26–28, 2021.
[16] PHYWE SYSTEME GmbH & Co. KG. Exp. Physics laboratory experiments catalogue—phywe. 2012. Available: https://studylib.net/doc/18036105/physics (accessed on 17 August 2026).
[17] Char M, Tilioua A. Toward high-performance green building: influence of geopolymer and straw fiber on mechanical and thermal performance. *Clean. Waste Syst.* 2025, 12:100327.
[18] Jonoobi M, Aitomaki Y, Mathew AP, Oksman K. Thermoplastic polymer impregnation of cellulose nanofibre networks: morphology, mechanical and optical properties. *Compos. Appl. Sci. Manuf.* 2014, 58:30–35.
[19] Mayandi K, Rajini N, Pitchipoo P, Jappes JW, Rajulu AV. Extraction and characterization of new natural lignocellulosic fiber Cyperus pangorei. *Int. J. Polym. Anal. Char.* 2016, 21:175–183.
[20] Ramli R, Khan MM, Yunus RM, Ong HR, Halim RM, *et al.* Insitu impregnation of copper nanoparticles on palm empty fruit bunch powder. *Adv. Nanopart.* 2014, 3(8):6571.
[21] Sheltami RM, Abdullah I, Ahmad A, Dufresne A, Kargarzadeh H. Extraction of cellulose nanocrystals from mengkuang leaves (Pandanus tectorius). *Carbohydr. Polym.* 2012, 88:772–779.
[22] Tserki V, Zafeiropoulos NE, Simon F, Panayiotou C. A study of the effect of acetylation and propionylation surface treatments on natural fibres. *Compos. Appl. Sci. Manuf.* 2005, 36(8):1110–1118.
[23] Liu Y, Thibodeaux D, Gamble G, Bauer P, VanDerveer D. Comparative investigation of Fourier transform infrared (FT-IR) spectroscopy and X-ray diffraction (XRD) in the determination of cotton fiber crystallinity. *Appl. Spectrosc.* 2012, 66(8):983–986.

[24] Qlihaa A, Dhimni S, Melrhaka F, Hajjaji N, Srhiri A. Caractérisation physico-chimique d'une argile marocaine physico-chemical characterization of a morrocan clay. *J. Mater. Environ. Sci.* 2016, 7:1741–1750.

[25] Martins MA, Kiyohara PK, Joekes I. Scanning electron microscopy study of raw and chemically modified sisal fibers. *J. Appl. Polym. Sci.* 2004, 94(6):2333–2340.

[26] Corrêa AC. Preparation of cellulose nanofibers from curauá fibers for the development of polymeric nanocomposites with EVA. Doctoral Thesis, Universidade Federal de São Carlos, 2010.

[27] Tomczak F. Studies on the structure and properties of coconut and curauá fibers from Brazil. Doctoral Thesis, Universidade Federal do Paraná, 2010.

[28] Dubis E, Dubis A, Morzycki J. Comparative analysis of plant cuticular waxes using HATR FT-IR reflection technique. *J. Mol. Struct.* 1999, 511:173–179.

[29] Krüger R. Cellulosic filament yarn from the NMMO process. *Lenz. Ver.* 1994, 74:49–52.

[30] Chaib H, Kriker A, Mekhermeche A. Thermal study of earth bricks reinforced by date palm fibers. *Energy Procedia* 2015, 74:919–925.

[31] Tayeh B, Hadzima-Nyarko M, Riad MY, Hafez RD. Behavior of ultrahigh-performance concrete with hybrid synthetic fiber waste exposed to elevated temperatures. *Buildings* 2023, 13(1):129.

[32] Awoyera PO, Akinrinade AD, de Sousa Galdino AG, Althoey F, Kirgiz MS, *et al*. Thermal insulation and mechanical characteristics of cement mortar reinforced with mineral wool and rice straw fibers. *J. Build. Eng.* 2022, 53(3):104568.

[33] Hakkoum S, Kriker A, Mekhermeche A. Thermal characteristics of model houses manufactured by date palm fiber reinforced earth bricks in desert regions of Ouargla Algeria. *Energy Procedia* 2017, 119:662–669.

[34] Taallah B, Guettala A. The mechanical and physical properties of compressed earth block stabilized with lime and filled with untreated and alkali-treated date palm fibers. *Constr. Build. Mater.* 2016, 104:52–62.

[35] Marandi SM, Bagheripour MH, Rahgozar R, Zare H. Strength and ductility of randomly distributed palm fibers reinforced silty-sand soils. *Am. J. Appl. Sci.* 2008, 5(3):209–220.

[36] Alshuhail K, Aldawoud A, Syarif J, Abdoun AI. Enhancing the performance of compressed soil bricks with natural additives: wood chips and date palm fibers. *Constr. Build. Mater.* 2021, 295:123611.

[37] Taallah B, Guettala A, Guettala S, Kriker A. Mechanical properties and hygroscopicity behavior of compressed earth block filled by date palm fibers. *Constr. Build. Mater.* 2014, 59:161–168.

[38] Cascone S, Rapisard R, Cascone D. Physical properties of straw bales as a construction material: a review. *Sustainability* 2019, 11(12):3388.

[39] Binici H, Aksogan O, Shah T. Investigation of fibre reinforced mud brick as a building material. *Constr. Build. Mater.* 2005, 19(4):313–318.

[40] Ashour T, Wieland H, Georg FJ, Bockisch FJ, Wu W. The influence of natural reinforcement fibres on insulation values of earth plaster for straw bale buildings. *Mater. Des.* 2010, 31(10):4676–4685.